of ϕ_1 and ϕ_2 becomes less important whereas the role of θ_1 and θ_2 increases (the trend from system 8 to system 6).

IV. Concluding Remarks

In this paper, we derived a rate theory for diffusive multidimensional barrier crossing that is valid for a moderate to high barrier and explicitly accounts for hydrodynamic interactions. The theory enables us to elucidate the detailed aspects of torsional dynamics in *n*-butane. The validity of the theory is confined to the high-friction regime where inertial effects can be neglected. Other major assumptions are the validity of the quadratic approximations for the potential energy in the neighborhood of the reactant, product, and transition states, zero-order approximations to the frictional tensor, and zero-curvature approximation for the reaction coordinate. The theory also fails for those reactions in which the reaction coordinate bypasses the saddle point significantly owing to a large frictional anisotropy.[49] The extension of the present theory to the lower friction regime should involve the use of the generalized Langevin equation rather than the simple Langevin equation employed in the present theory; in the low-friction regime, the passage through the barrier region occurs rapidly and thus a memory effect in the interactions with the solvent medium can play a role. If memory effects can be neglected, the present theory can be easily extended to lower friction regime for systems of identical particles in the free-draining limit[31] (see section IIB). We have applied the present theory to investigate the kinetics of conformational transitions in long alkane chains.[50] The results are in good agreement with those of ref 28 and 38 and give us further confidence in the present rate theory. Applications to other systems are the subjects of future work.

Acknowledgment. We thank Dr. B. M. Pettitt and Dr. C. L. Brooks III for a critical reading of the manuscript and an anonymous referee for valuable comments.

Appendix. Boundary Values of s-Coordinates

We should first determine the optimum locations of the barrier region boundaries along the coordinate q_r by use of (2.89) or (2.90); as introduced under section IIB, q_r is the coordinate in terms of which the barrier crossing process is defined (e.g., in the case of conformational isomerization in *n*-butane treated under section III, the dihedral angle ϕ_4 corresponds to q_r). The values of reactive *s*-coordinates at the boundaries can be evaluated from

$$\mathbf{s}^\alpha = \boldsymbol{D}_\alpha^{-1}\cdot\boldsymbol{C}_\alpha^{-1}\cdot\boldsymbol{B}_\alpha^{-1}\cdot\mathbf{q}^\alpha \qquad \text{(A.1)}$$

where α denotes the quantities associated with barrier region (α = *), reactant region (α = R), and product region (α = P). However, since we do not know the values of q^α-coordinates at R* and P* except for q_r^α, the procedure is not straightforward. If the reaction coordinate follows q_r^α strictly, we may set the values of the other q^α-coordinates equal to zero at R* and P*. But this is not the case in general. To evaluate the values of s_i^α at the boundaries, we take the values of the other *s*-coordinates, s_j^α ($j \neq i$), to be zeros. Then, (A.1) represents a system of f linear equations with f unknowns $\{s_i^\alpha, q_1^\alpha, \ldots, q_{r-1}^\alpha, q_{r+1}^\alpha, \ldots, q_f^\alpha\}$. Solving (A.1) for these unknowns, we get the boundary values of s_i^α. The values of q_i^α (i=1, ..., r-1, r+1, ..., f) obtained in this way, together with the boundary value of q_r^α, give the representation of the normal mode s_i^α in terms of q^α-coordinates.

Registry No. Butane, 106-97-8.

(49) For an example in which the frictional anisotropy dominates to make the reaction pathway bypass the saddle point, see Northrup, S. H.; McCammon, J. A. *J. Chem. Phys.* **1983**, *78*, 987.
(50) Lee, S.; Karplus, M., in preparation.

Why Does Intersystem Crossing Occur in Isolated Molecules of Benzaldehyde, Acetophenone, and Benzophenone?

Nobuaki Ohmori, Toshinori Suzuki, and Mitsuo Ito*

Department of Chemistry, Faculty of Science, Tohoku University, Sendai 980, Japan *(Received: July 27, 1987; In Final Form: November 16, 1987)*

The sensitized phosphorescence excitation spectra of jet-cooled benzaldehyde, acetophenone, and benzophenone have been measured. Well-resolved vibrational structures were found in the $S_1(n,\pi^*) \leftarrow S_0$ and $T_1(n,\pi^*) \leftarrow S_0$ spectra of all molecules. The $T_1(n,\pi^*)$ state is located 1500–2000 cm^{-1} below the $S_1(n,\pi^*)$ state. Some signs were obtained showing the presence of a second triplet state, possibly $T(\pi,\pi^*)$, near $T_1(n,\pi^*)$ for benzaldehyde and acetophenone. The results obtained for the isolated molecules raise a question as to the mechanism for the efficient S_1–T intersystem crossing in these molecules.

Introduction

The intersystem crossing of aromatic ketones and aldehydes such as benzaldehyde, acetophenone, and benzophenone has been studied extensively, mainly in the condensed phase. The lowest excited singlet states of these molecules are $S_1(n,\pi^*)$. It is believed that there exist two triplet states, $T(n,\pi^*)$ and $T(\pi,\pi^*)$, below $S_1(n,\pi^*)$ and these lie close to each other in the $\sim$2000-cm^{-1} energy gap between S_1 and the lowest triplet state. The presence of these two triplet states is suggested by the phosphorescence excitation experiments of Case and Kearns[1] in acetophenone, and by similar experiments on benzaldehyde by Hayashi and Nagakura.[2] The existence of the two triplet states was also shown by Migirdicyan from the observation of the phosphorescence spectra from both $T(n,\pi^*)$ and $T(\pi,\pi^*)$ for 2,4,5-trimethylbenzaldehyde in durene.[3] Electron spin resonance studies also provide strong evidence for the existence of nearby $T(n,\pi^*)$ and $T(\pi,\pi^*)$ states in these molecules.[4] All the results so far available leave little room for doubt of the presence of $T(\pi,\pi^*)$ below $S_1(n,\pi^*)$ in the condensed phase. It is well-known that this triplet state could play an essential role in the efficient intersystem crossing of these molecules.

The efficient intersystem crossing from $S_1(n,\pi^*)$ to $T(\pi,\pi^*)$ in the condensed phase[6] despite their small energy separation can be understood by assuming that dense vibrational states supplied

(1) Case, W. A.; Kearns, D. R. *J. Chem. Phys.* **1970**, *52*, 2175.
(2) Hayashi, H.; Nagakura, S. *Mol. Phys.* **1974**, *27*, 969.
(3) Migirdicyan, E. *Chem. Phys. Lett.* **1972**, *12*, 473.
(4) Hayashi, H.; Nagakura, S. *Chem. Phys. Lett.* **1973**, *18*, 63. Cheng, T. H.; Hirota, N. *Mol. Phys.* **1974**, *27*, 281. Mao, S. W.; Hirota, N. *Mol. Phys.* **1974**, *27*, 309. Harrigan, E. T.; Hirota, N. *Mol. Phys.* **1976**, *663*, 681.
(5) El-Sayed, M. A. *J. Chem. Phys.* **1963**, *38*, 2834.
(6) Lamda, A. A.; Hammond, G. S. *J. Chem. Phys.* **1965**, *43*, 2129.

0022-3654/88/2092-1086$01.50/0

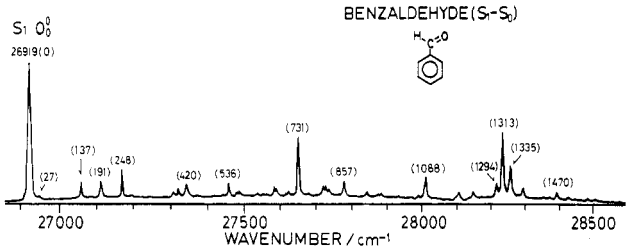

Figure 1. Sensitized phosphorescence excitation spectrum of jet-cooled benzaldehyde in $S_1 \leftarrow S_0$ region.

from phonons of the environment play a significant role. In the isolated molecule in which phonons are absent, the density of intramolecular vibrational states of $T(\pi,\pi^*)$ isoenergetic with $S_1(n,\pi^*)$ is not large enough for efficient intersystem crossing if the energy separation between $S_1(n,\pi^*)$ and $T(\pi,\pi^*)$ is the same order as that in the condensed phase. Therefore, it is of particular interest to determine where $T(\pi,\pi^*)$ is located in the isolated molecule.

Toward this end, we report here the sensitized phosphorescence excitation spectra of jet-cooled benzaldehyde, acetophenone, and benzophenone due to the $S_1 \leftarrow S_0$ and $T \leftarrow S_0$ transitions. We have obtained some signs of the presence of $T(\pi,\pi^*)$ near $T(n,\pi^*)$ for benzaldehyde and acetophenone although the location of $T(\pi,\pi^*)$ was not determined. The result raises a question as to the mechanism of intersystem crossing in the isolated molecule, a question that is discussed here in some detail.

Experimental Section

The experimental apparatus for sensitized phosphorescence excitation spectroscopy has been described elsewhere.[7] A gaseous mixture of the sample vapor and He was expanded into a vacuum chamber at 1×10^{-4} Torr through a pulsed nozzle of 0.8 mm diameter. A tunable dye laser (Lambda Physik FL-2002) pumped by a Xe–Cl excimer laser (Lambda Physik EMG-102MSC) was used as an exciting light source. The laser beam crossed the jet 10 mm downstream and the molecule in the jet was directly excited to its S_1 and T states.

The phosphorescence excitation spectrum was measured by probing the sensitized phosphorescence emitted from a solid phosphor surface on which the triplet-state molecule is deposited. For the $S_1 \leftarrow S_0$ spectra, the triplet-state molecule was produced from S_1 by intersystem crossing, while for the $T \leftarrow S_0$ spectra, the triplet-state molecule was directly produced by $T \leftarrow S_0$ absorption. The triplet-state molecules travel for 40 μs from the excitation position and collide with a liquid nitrogen cooled copper surface installed 80 mm downstream from the nozzle. The cold surface is covered with the sample itself, which serves as a phosphor. When the triplet-state molecules in the jet collide with the solid phosphor, energy transfer occurs and sensitized phosphorescence is emitted. The use of the solid sample itself seems to be suitable for efficient energy transfer. The phosphorescence was detected by a photomultiplier (HTV R585) which was cooled at −20 °C, and the signal was counted by a photon-counting system (Ortec 9302, 9315, 9325 in the gated mode) with a 30-ms gate width after a 50-μs delay from the laser fire.

Benzaldehyde, acetophenone, and benzophenone were obtained from Tokyo Kasei. Benzaldehyde and acetophenone were purified by vacuum distillation, and benzophenone was purified by vacuum sublimation.

Results and Discussion

Benzaldehyde. Figure 1 shows the sensitized phosphorescence excitation spectrum of jet-cooled benzaldehyde in the region of the $S_1 \leftarrow S_0$ transition. Table I lists the main vibronic bands. The $S_1 \leftarrow S_0$ spectrum is characterized by an intense origin band at 26 919 cm^{-1} and a vibronic band involving the excited-state C=O stretching mode of 1313 cm^{-1}. The strong appearance of the C=O stretching mode supports the assignment of S_1 as an (n,π^*) state. The position of the origin agrees very well with that reported for the vapor (26 923 cm^{-1}),[8] but is red shifted by 365 cm^{-1} from the value reported in a *p*-dibromobenzene matrix (27 284 cm^{-1}).[2] The vibrational structure does not have much regularity, and its detailed analysis is not attempted here. However, several points may be worth mentioning. The absence of prominent progression except for the carbonyl progression (which was observed in the vapor absorption spectrum)[8] implies no great difference in the geometrical structure between $S_1(n,\pi^*)$ and S_0 except for the C=O distance. The lowest frequency vibrational mode of benzaldehyde is the torsion of the C–CHO bond; its frequency is 110 cm^{-1} in S_0.[9] This mode appears very weakly in hot bands on the lower frequency side of the 0_0^0 band, as seen at the high-frequency end of Figure 2. The corresponding excited-state frequency was found

TABLE I: Phosphorescence Excitation Spectrum of Benzaldehyde in $S_1 \leftarrow S_0$ Region

ν/cm^{-1}	$\nu - \nu(0_0^0)$/cm^{-1}	rel int	assignt[a]
26 809	−110	0.7	36_1^0
26 832	−87	0.8	
26 893	−26	3	$25_1^1 36_1^1$
26 919	0	100	$S_1(n,\pi^*)0_0^0$
26 946	27	3	36_1^1
27 056	137	13	36_0^1
27 110	191	14	
27 167	248	24	
27 192	273	2	
27 302	383	4	
27 316	397	7	
27 339	420	10	
27 438	519	1	
27 455	536	12	
27 477	558	3	
27 483	564	4	
27 531	612	2	
27 549	630	2	
27 558	639	2	
27 580	661	8	
27 587	668	6	
27 615	696	2	
27 621	702	4	
27 650	731	48	ring
27 676	757	1	
27 717	798	9	
27 728	809	8	
27 733	814	6	
27 776	857	13	
27 840	921	4	
27 870	951	2	
27 881	962	4	
27 915	996	1	
27 930	1011	2	
27 986	1067	2	
28 007	1088	18	C–C stretch
28 093	1174	2	
28 101	1182	6	
28 144	1225	5	
28 213	1294	12	
28 232	1313	53	C=O stretch
28 254	1335	26	
28 277	1358	8	
28 292	1373	7	
28 350	1431	2	
28 360	1441	1	
38 369	1450	1	
28 389	1470	6	
28 423	1504	2	
28 445	1526	1	
28 461	1542	1	
28 479	1560	3	
28 501	1582	1	

[a] Mode notation is taken from ref 10.

(7) Abe, H.; Kamei, S.; Mikami, N.; Ito, M. *Chem. Phys. Lett.* **1984**, *109*, 217.
(8) Imanishi, S.; Semba, K.; Ito, M.; Anno, T. *Bull. Chem. Soc. Jpn.* **1952**, *25*, 150.
(9) Miller, F. A.; Fateley, W. G.; Witkowski, R. E. *Spectrochim. Acta, Part A* **1967**, *23A*, 891.

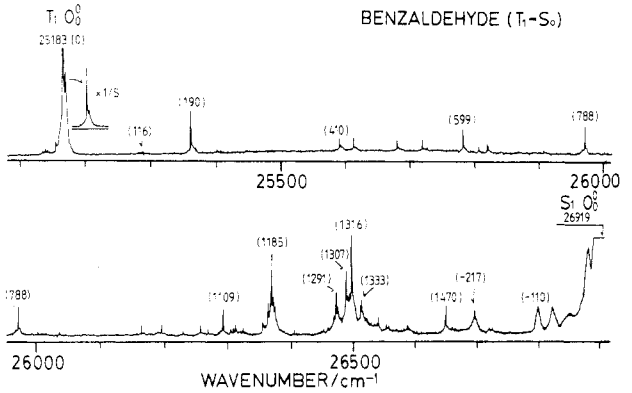

Figure 2. Sensitized phosphorescence excitation spectrum of jet-cooled benzaldehyde in T ← S_0 region.

to be 137 cm^{-1}, because of the presence of a vibronic band at 137 cm^{-1} and also of a sequence band due to the 1–1 transition of the torsional mode at 27 cm^{-1} (137–110 cm^{-1}) above the 0_0^0 band. The higher frequency of the torsional mode in S_1 indicates an increase of π-conjugation between the phenyl and CHO groups in the transition from S_0 to S_1. All of the vibronic bands in the S_1 ← S_0 spectrum exhibit a similar band shape with the half-width of about 4 cm^{-1}. This fairly large width is in marked contrast to the bandwidths found in the T ← S spectrum, which will be described below.

Figure 2 shows the sensitized phosphorescence excitation spectrum of jet-cooled benzaldehyde in the ~2000-cm^{-1} region below the S_1 origin; the "T ← S_0" spectrum. The intensity of this spectrum is weaker by a factor of 10^2 than the intensity of the S_1 ← S_0 spectrum. The T ← S_0 spectrum consists of many vibronic bands which are extremely sharp. The half-width was found to be about 0.4 cm^{-1} from high-resolution measurements. The main vibronic bands are given in Table II. The lowest frequency strong band at 25 183 cm^{-1} is assigned as the origin of the spectrum. This frequency is in agreement with that of the origin band in the vapor phosphorescence spectrum reported by Koyanagi and Goodman[10] and by Hollas and Thakur.[11] The vibrational structure qualitatively corresponds to that of $S_1(n,\pi^*)$ ← S_0: the strong vibronic bands involving the C=O stretching mode of 1316 cm^{-1} (1313 cm^{-1} in S_1 ← S_0), the C—C stretching mode of 1185 cm^{-1} (1088 cm^{-1} in S_1 ← S_0), the ring mode of 788 cm^{-1} (731 cm^{-1} in S_1 ← S_0), and the in-plane CHO bending mode of 190 cm^{-1} [10] (191 or 248 cm^{-1} in S_1 ← S_0). Although there are some detailed differences between the T ← S_0 and S_1 ← S_0 spectra, their gross similarity suggests that the T state is a counterpart of $S_1(n,\pi^*)$ having the same electron configuration, that is, T-(n,π^*). In their phosphorescence excitation study of benzaldehyde in the *p*-dibromobenzene matrix at 4.2 K, Hayashi and Nagakura[2] located the origin of $T(n,\pi^*)$ at 25 515 cm^{-1}. The origin of the isolated molecule is red shifted from the origin in the matrix by 332 cm^{-1}, which is nearly equal to the corresponding shift for S_1 ← S_0. Therefore, it is concluded that the band at 25 183 cm^{-1} is the 0_0^0 band of $T(n,\pi^*)$ ← S_0. The energy difference between the origins of $S_1(n,\pi^*)$ ← S_0 and $T(n,\pi^*)$ ← S_0 is 1736 cm^{-1}, which is nearly equal to the value of 1769 cm^{-1} in the low-temperature matrix.

Hayashi and Nagakura[2] reported $T_1(\pi,\pi^*)$ to be located at 25 332 cm^{-1} in the *p*-dibromobenzene matrix at 4.2 K, which is 183 cm^{-1} below the origin of $T_2(n,\pi^*)$ in the matrix. We searched for bands due to $T(\pi,\pi^*)$ ← S_0 for the jet-cooled molecule over a wide spectral region below the origin of $T(n,\pi^*)$. Under our experimental conditions, we should have been able to detect a band whose intensity is larger than $^1/_{50}$ of the intensity of the origin of $T(n,\pi^*)$. However, no band was found anywhere in the 1000-cm^{-1} region below the $T(n,\pi^*)$ origin. This result shows that the intensity of $T(\pi,\pi^*)$ ← S_0 is about 2 orders of magnitude weaker than $T(n,\pi^*)$ ← S_0, if the former is located in the region studied. According to the matrix spectrum reported by Hayashi and Nagakura,[2] the intensity of $T_1(\pi,\pi^*)$ ← S_0 is larger than $^1/_{10}$ of the intensity of $T_2(n,\pi^*)$ ← S_0. The large intensity of the former is probably ascribed to the external heavy atom effect, which is known to be larger for (π,π^*) states than (n,π^*) states.

Since the energy ordering of the triplet states of aromatic ketones and aldehydes is easily inverted by solvent perturbations,[12]

TABLE II: Phosphorescence Excitation Spectrum of Benzaldehyde in T ← S_0 Region

ν/cm^{-1}	$\nu - \nu(0_0^0)$/cm^{-1}	rel int	assign[a]
24 967	−216	1	36_2^0
25 153	−30	2	25_1^1
25 157	−26	2	$25_1^1 36_1^1$
25 160	−23	2	
25 173	−10	4	35_1^1
25 183	0	100	$T(n,\pi^*)0_0^0$
25 187	4	28	36_1^1
25 299	116	1	36_0^2
25 373	190	14	
25 411	228	1	
25 416	232	1	
25 593	410	4	
25 615	432	5	
25 681	498	4	
25 719	536	4	
25 782	599	8	
25 807	624	2	
25 820	637	3	
25 822	639	2	
25 907	724	1	
25 972	789	11	ring
26 003	820	1	
26 035	849	1	
26 072	889	1	
26 156	973	4	
26 195	1012	4	
26 229	1046	1	
26 256	1073	3	
26 268	1085	2	
26 292	1109	8	
26 304	1121	2	
26 309	1126	2	
26 312	1129	3	
26 325	1142	2	
26 355	1172	4	
26 362	1179	11	
26 368	1185	27	C–C stretch
26 370	1187	13	
26 374	1191	10	
26 377	1194	5	
26 384	1201	2	
26 405	1222	1	
26 454	1271	1	
26 460	1277	2	
26 471	1288	6	
26 474	1291	16	
26 477	1294	9	
26 490	1307	21	
26 499	1316	50	C=O stretch
26 514	1331	10	
26 516	1333	12	
26 522	1339	6	
26 525	1342	5	
26 542	1359	6	
26 556	1373	3	
26 559	1376	3	
26 590	1407	3	
26 654	1470	12	
26 665	1482	2	
26 702	−217	10	36_2^0
26 809	−110	15	36_1^0
26 919	0	~2 × 10^3	$S_1(n,\pi^*)0_0^0$

[a] Mode notation is taken from ref 10.

(10) Koyanagi, M.; Goodman, L. *Chem. Phys.* **1979**, *39*, 237.
(11) Hollas, J. M.; Thakur, S. N. *Chem. Phys.* **1973**, *1*, 385.
(12) Zwarich, R. J.; Goodman, L. *Chem. Phys. Lett.* **1970**, *7*, 609. Koyanagi, M.; Zwarich, R. J.; Goodman, L. *Chem. Phys. Lett.* **1970**, *9*, 74. Goodman, L.; Koyanagi, M. *J. Chem. Phys.* **1972**, *57*, 1809.

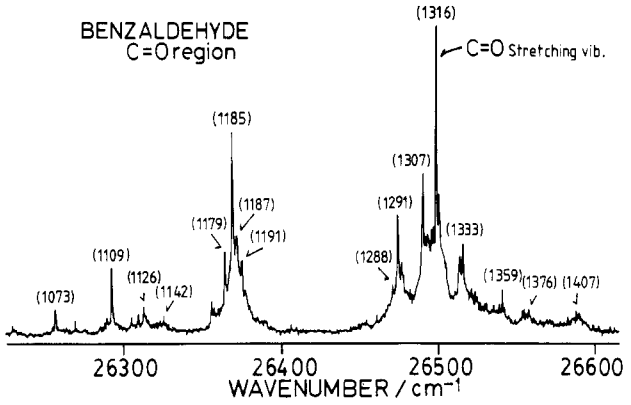

Figure 3. Spectrum of Figure 2 in the region 26 200–26 600 cm^{-1} on an expanded scale.

it is quite possible that $T(\pi,\pi^*)$ is located above $T(n,\pi^*)$ in the isolated molecule. However, all the vibronic bands including very weak ones in Figure 2 have the same band shape as that of the origin of $T_1(n,\pi^*)$ and no band is found whose band shape is different as expected for bands belonging to $T(\pi,\pi^*)$. A marked feature of Figure 2 is that the vibronic bands are rather sparse in the region from the origin of $T(n,\pi^*)$ up to the excess vibrational frequency of $\sim$1000 cm^{-1}, but in the region beyond 1000 cm^{-1}, the bands are heavily congested, especially around the strong bands at 1180 and 1300 cm^{-1} (see Figure 3). The heavy congestion is readily recognized by comparison with the same vibrational region of $S_1(n,\pi^*) \leftarrow S_0$ in Figure 1, where such a band congestion is not seen. The appearance of many vibronic bands in $T(n,\pi^*) \leftarrow S_0$ (about 30 bands between 1000 and 1350 cm^{-1}) and a smaller number of bands in $S_1(n,\pi^*) \leftarrow S_0$ (about 15 bands between 1000 and 1350 cm^{-1}) might be an apparent result, ascribed to differences in their intrinsic band widths. However, such a difference is not observed between the vibronic bands of the two spectra in the region of excess vibrational energy less than 1000 cm^{-1} (about 20 and 30 bands, respectively, for $T_1(n,\pi^*) \leftarrow S_0$ and $S_1(n,\pi^*) \leftarrow S_0$). Therefore, we believe that in $T_1(n,\pi^*) \leftarrow S_0$ about 10 extra bands newly appear in the region from 1000 to 1350 cm^{-1}.

The extra bands appearing around the intense vibronic bands might be assigned to the vibronic bands of $T(\pi,\pi^*) \leftarrow S_0$. Although the vibronic bands of $T(\pi,\pi^*) \leftarrow S_0$ will be extremely weak, they can appear by borrowing intensity from nearby $T(n,\pi^*)$ vibronic levels by a vibrationally induced breakdown of the Born–Oppenheimer approximation.[13] If we try to explain the appearance of these extra bands by intensity borrowing, the number of vibronic levels of $T(\pi,\pi^*)$ in the energy region corresponding to 1000–1300 cm^{-1} of $T(n,\pi^*)$ should be considerably large. On the other hand, the sparse feature of the spectrum in the region less than 1000 cm^{-1} suggests that the vibronic levels of $T(\pi,\pi^*)$ in the corresponding region are rather sparse. It follows, then, that the origin of $T(\pi,\pi^*)$ lies not far from the origin of $T(n,\pi^*)$. There exist several sharp bands just near the origin band of $T(n,\pi^*)$ (see Table II). Assuming that these bands also occur by intensity borrowing with some $T(\pi,\pi^*)$ vibronic levels, the origin of $T(\pi,\pi^*)$ should be located below the origin of $T(n,\pi^*)$. However, these bands can be reasonably assigned as 1–1 transitions of low-frequency modes.[10,11] The fact that the origin band of the vapor phosphorescence spectrum[9,10] coincides with the origin of $T(n,\pi^*)$ supports that $T(n,\pi^*)$ is the lowest triplet state. After all, we think that the origin of $T(\pi,\pi^*)$, if any, lies above the origin of $T(n,\pi^*)$ but not far from the latter.

Acetophenone. Figure 4 shows the sensitized phosphorescence excitation spectrum of jet-cooled acetophenone due to the $S_1(n,\pi^*) \leftarrow S_0$ transition. The main vibronic bands are listed in Table III. The longest wavelength, prominent band at 27 279 cm^{-1} is taken as the band origin. On the higher frequency side of the 0_0^0 band, several low-frequency strong bands appear with displacements of 38, 68, and 92 cm^{-1} from the origin. These bands have been

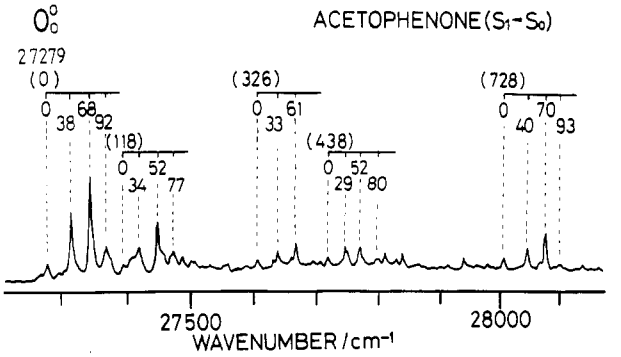

Figure 4. Sensitized phosphorescence excitation spectrum of jet-cooled acetophenone in $S_1 \leftarrow S_0$ region. Bands associated with internal rotation of the methyl group are indicated.

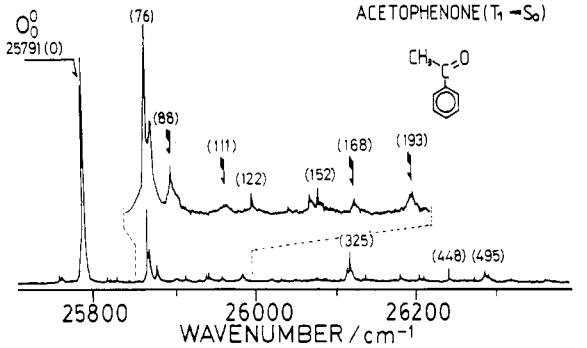

Figure 5. Sensitized phosphorescence excitation spectrum of jet-cooled acetophenone in $T \leftarrow S_0$ region. Spectrum in the region 70–200 cm^{-1} is shown on an expanded scale. Bands indicated by arrows are broad bands.

assigned in a previous paper[14] to the levels associated with the internal rotation of the methyl group in S_1. The frequencies of 38, 68, and 92 cm^{-1} represent the 2e, $3a_1$, and 4e levels in the usual notation of the internal rotation levels. The height of barrier to the internal rotation is roughly estimated to be 30 cm^{-1} in S_1. It is also suggested from the observed intensity pattern that the most stable conformation of the CH_3 group with respect to the molecular framework is quite different between S_0 and S_1. The bands including the 0_0^0 band form a structural unit, and a similar structural unit repeatedly appears in combination with vibronic bands at displacements of 118, 326, 438, 728, and 1186 cm^{-1}. The frequency intervals in each structural unit are nearly equal to those belonging to the 0_0^0 band except for the vibronic bands of 118 and 438 cm^{-1}. The frequency intervals for the latter are 30, 52, and 78 cm^{-1}, smaller than those for the 0_0^0 band. Since 438 cm^{-1} is nearly equal to 118 + 326 cm^{-1}, the vibronic bands of 118 and 438 appear to involve a common mode of 118 cm^{-1}. The large difference in the internal rotational levels associated with the mode of 118 cm^{-1} clearly indicates a strong coupling of the internal rotation with this low-frequency mode.

The vibrational structure of the $S_1(n,\pi^*) \leftarrow S_0$ spectrum of jet-cooled acetophenone is similar to that of benzaldehyde except for the appearance of the vibronic bands associated with the internal rotation and apparent absence of a strong band involving the C=O stretching mode. Case and Kearns[1] explained the absence of the carbonyl band by an extensive mixing of the carbonyl mode with other modes having similar frequencies. In the acetophenone crystal,[1] the origin of $S_1(n,\pi^*) \leftarrow S_0$ is reported to be at 27 941 cm^{-1}, which may be compared with 27 279 cm^{-1} for the isolated molecule. Therefore, a blue shift as large as 662 cm^{-1} is induced by the crystal field.

Figure 5 shows the sensitized phosphorescence excitation spectrum of jet-cooled acetophenone in the $T \leftarrow S_0$ region. The intensity of this spectrum is $^1/_{20}$ of that of the $S_1(n,\pi^*) \leftarrow S_0$

(13) Hochstrasser, R. M.; Marzzaro, C. *J. Chem. Phys.* **1968**, *49*, 971.

(14) Kamei, S.; Okuyama, K.; Abe, H.; Mikami, N.; Ito, M. *J. Phys. Chem.* **1986**, *90*, 93.

TABLE III: Phosphorescence Excitation Spectrum of Acetophenone in $S_1 \leftarrow S_0$ Region

ν/cm^{-1}	$\nu - \nu(0_0^0)$/cm^{-1}	rel int	assignt
27 061	−218	2	
27 100	−178	2	
27 119	−160	4	
27 169	−110	14	
27 218	−61	8	
27 229	−50	6	
27 268	−11	33	
27 279	0	100	$S_1(n,\pi^*)0_0^0$
27 297	18	16	
27 305	26	20	
27 317	38	370	0_0^0 + 2e
27 347	68	580	0_0^0 + $3a_1$
27 371	92	150	0_0^0 + 4e
27 397	118	65	118
27 411	132	110	
27 421	142	170	118 + 2e
27 449	170	280	118 + $3a_1$
27 469	190	63	
27 474	195	83	118 + 4e
27 487	208	62	
27 501	222	39	
27 507	228	41	
27 518	239	12	
27 530	251	24	
27 558	279	40	
27 574	295	22	
27 590	311	27	
27 605	326	57	326
27 631	352	43	
27 638	359	90	326 + 2e
27 659	380	50	
27 667	388	130	326 + $3a_1$
27 693	414	30	326 + 4e
27 705	426	28	
27 717	438	54	438 (118 + 326)
27 746	467	110	438 + 2e
27 769	490	120	438 + $3a_1$
27 797	518	30	
27 809	530	65	
27 828	549	41	
27 838	559	74	
27 861	582	18	
27 913	634	25	
27 940	661	65	
27 961	682	17	
27 980	701	24	
28 007	728	71	728
28 047	768	140	728 + 2e
28 077	798	230	728 + $3a_1$
28 100	821	38	728 + 4e
28 109	830	12	
28 130	851	13	
28 138	859	25	
28 167	888	20	
28 197	918	38	
28 240	961	12	
28 249	970	34	
28 276	997	60	
28 320	1041	25	
28 379	1100	13	
28 430	1151	19	
28 456	1177	12	
28 465	1186	16	1186
28 502	1223	60	1186 + 2e
28 531	1252	97	1186 + $3a_1$
28 555	1276	10	1186 + 4e
28 568	1289	13	
28 635	1356	42	

spectrum. The frequencies of the bands are listed in Table IV. Similar to the case of benzaldehyde, main vibronic bands are extremely sharp with the strongest sharp band lying at 25 791 cm^{-1}. This spectrum gradually loses its intensity with an increase of excess vibrational frequency and disappears in the region beyond 500 cm^{-1}. The band at 25 791 cm^{-1} is assigned to the origin of

TABLE IV: Phosphorescence Excitation Spectrum of Acetophenone in $T \leftarrow S_0$ Region

ν/cm^{-1}	$\nu - \nu(0_0^0)$/cm^{-1}	rel int[a]	assignt
25 763	−28	3 s	
25 765	−26	3 s	
25 791	0	100 s	$T(n,\pi^*)0_0^0$
25 792	1	63 s	
25 867	76	38 s	torsion
25 869	78	19 s	
25 879	88	10 b	
25 902	111	2 b	
25 913	122	4 s	
25 930	139	1 s	
25 939	148	4 s	
25 943	152	5 s	
25 595	168	3 b	
25 984	193	4 b	
26 019	228	2 b	
26 030	239	2 s	
26 048	257	1	
26 073	282	1	
26 082	291	1	
26 085	294	2	
26 112	321	7 s	
26 116	325	17 s	
26 134	343	4 s	
26 177	387	4 s	
26 201	410	4 s	
26 207	416	3 s	
26 239	448	7 s	
26 285	494	6 b	
26 318	527	2	
26 362	571	2	
26 538	747	3 vb	
26 552	761	4 vb	
26 566	775	3 vb	
26 665	874	3 vb	
26 758	967	4 vb	
26 801	1010	4 vb	
26 918	1127	6 vb	
26 947	1156	3 vb	
26 980	1189	5 vb	
26 992	1201	7 vb	
27 014	1223	2 vb	
27 032	1241	2 vb	
27 061	1270	7 vb	
27 077	1286	3 vb	
27 100	1309	6 vb	
27 119	1328	11 vb	
27 127	1336	9 vb	
27 146	1355	7 vb	
27 156	1365	8 vb	
27 169	1378	40 vb	
27 183	1392	8 vb	
27 218	1427	8 vb	
27 229	1438	7 vb	
27 279	1488	300 vb	$S_1(n,\pi^*)0_0^0$

[a] s,b, and vb indicate sharp, broad, and very broad bands, respectively. The very broad bands are ovbiously hot bands belonging to $S_1(n,\pi^*)$.

the spectrum. Case and Kearns[1] reported the origin of $T(n,\pi^*) \leftarrow S_0$ transition in the crystal to be 26 396 cm^{-1}. The blue shift in the crystal is as large as 604 cm^{-1}, which is comparable with that (662 cm^{-1}) for $S_1(n,\pi^*) \leftarrow S_0$. The good correspondence with the crystal spectrum and a large intensity of the longest wavelength band of the jet spectrum show that the band at 25 791 cm^{-1} is the 0_0^0 band of the $T(n,\pi^*) \leftarrow S_0$ transition. The sharp bands appearing within the 500-cm^{-1} region on the higher frequency side of the 0_0^0 band are assigned to vibronic bands belonging to $T(n,\pi^*)$. Many bands seen in the excess vibrational frequency region 1000–1400 cm^{-1} (see Table IV) are obviously hot bands belonging to $S_1(n,\pi^*)$, which appear as a result of a great increase of the detection sensitivity required for the observation of the very weak $T \leftarrow S_0$ spectrum.

With a hope of finding bands due to $T(\pi,\pi^*) \leftarrow S_0$, a careful search was extended to 600 cm^{-1} below the origin of $T(n,\pi^*)$. No

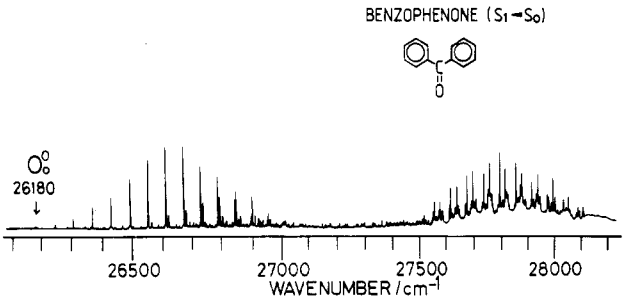

Figure 6. Sensitized phosphorescence excitation spectrum of jet-cooled benzophenone in $S_1 \leftarrow S_0$ region.

additional sharp bands were found. A careful inspection of Figure 5 reveals, however, that there are weak but broad bands whose shape is apparently different from that of the sharp band assigned to $T(n,\pi^*)$. The broad bands are indicated by arrows in the figure. They might be vibronic bands belonging to $T(\pi,\pi^*)$ although we have no positive evidence other than the band shape. We also notice the splitting of the origin of $T(n,\pi^*)$ into two sharp components. A similar splitting may also be observed for the vibronic band at 76 cm^{-1}. The splitting might arise from the interaction between the vibronic levels of $T(n,\pi^*)$ and $T(\pi,\pi^*)$. The interaction may also be reflected by the irregular vibrational structure of the $T \leftarrow S_0$ spectrum. In the acetophenone crystal, the lowest excited triplet state is $T_1(\pi,\pi^*)$, which is located about 300 cm^{-1} below the origin of $T(n,\pi^*)$ in the crystal. Our experimental results for the jet-cooled molecule seem to be consistent with the crystal result as far as the order of the two triplet states is concerned. However, since the order is known to be easily inverted by external perturbations, we have to reserve the conclusion. The only thing we can safely say is that the position of $T(\pi,\pi^*)$ is not far from $T(n,\pi^*)$.

A brief remark will be made here about the vibrational structure of $T(n,\pi^*) \leftarrow S_0$. The structure near the origin is quite different from that near the origin of $S_1(n,\pi^*) \leftarrow S_0$. In the latter, the 0_0^0 band is relatively weak and the bands associated with internal rotation of the methyl group have stronger intensities. In contrast, the 0_0^0 band of $T(n,\pi^*) \leftarrow S_0$ is the strongest band and there is no other strong band except for the one at 76 cm^{-1}. The band at 76 cm^{-1} is probably assigned to the torsion of the C–$COCH_3$ bond, which has a frequency of 48 cm^{-1} in S_0.[9] Therefore, in the $T(n,\pi^*) \leftarrow S_0$ spectrum of acetophenone, bands associated with internal rotation of the methyl group are absent or very weak. This means that both the potential of the internal rotation and the most stable conformation of the methyl group are similar in the $T_1(n,\pi^*)$ and S_0 states. As described before, the most stable conformation of the methyl group in $S_1(n,\pi^*)$ is greatly different from that in S_0. Therefore, $S_1(n,\pi^*)$ and $T_1(n,\pi^*)$ are greatly different with respect to orientation of the methyl group. It is remarkable that the singlet and triplet counterparts arising from the same electron configuration have such a difference in the geometrical structure.

Benzophenone. Figure 6 shows the sensitized phosphorescence excitation spectrum of jet-cooled benzophenone in the region of the $S_1(n,\pi^*) \leftarrow S_0$ transition. The spectrum is essentially the same as that reported in a previous paper,[15] but the S/N ratio is much improved in the present spectrum. As a result of an increase in the S/N ratio, a longest wavelength weak band at 26 180 cm^{-1} was newly found. This band, previously observed by Holtzclaw and Pratt,[16] is red shifted by one quantum of the in-phase torsional mode of 63 cm^{-1} from the band at 26 243 cm^{-1}, which was previously assigned by us as the origin of the spectrum. We also found a very weak band at 26 281 cm^{-1}, which is the first member of progression of the out-of-phase torsional mode of 101 cm^{-1} starting from the band at 26 180 cm^{-1}. Because of these newly found weak bands, revision of our earlier assignments should be made. The origin of the spectrum is at 26 180 cm^{-1}, and all quantum numbers n of the progressions of the torsional modes given in the previous paper should be read as $n + 1$. This revision does not impose any change in the vibrational analysis and interpretation developed there. The main vibronic bands and revised assignments are given in Table V.

The $S_1(n,\pi^*) \leftarrow S_0$ spectrum of jet-cooled benzophenone is characterized by long progressions of the in-phase torsional mode of 60 cm^{-1} appearing in the region 26 200–27 100 cm^{-1} and in the region 27 500–28 200 cm^{-1}. The latter is the C=O stretching region. It was shown from a detailed analysis of the spectrum that the dihedral angle of the two phenyl groups of the molecule

TABLE V: Phosphorescence Excitation Spectrum of Benzophenone in $S_1 \leftarrow S_0$ Region

ν/ cm^{-1}	$\nu - \nu(0_0^0)$/ cm^{-1}	rel int	assignt[a]	ν/ cm^{-1}	$\nu - \nu(0_0^0)$/ cm^{-1}	rel int	assignt[a]
26 180	0	1	$S_1(n,\pi^*)0_0^0$	26 847	667	95	$\alpha_0^8\beta_0^2$
26 243	63	7	α_0^1	26 897	717	46	α_0^{12}
26 281	101	1	β_0^1	26 902	722	146	$\alpha_0^9\beta_0^2$
26 305	125	29	α_0^2	26 910	730	45	
26 343	163	3	$\alpha_0^1\beta_0^{01}$	26 923	743	39	
26 367	187	77	α_0^3	26 951	771	13	α_0^{13}
26 380	200	2	β_0^2	26 957	777	85	$\alpha_0^{10}\beta_0^2$
26 404	224	8	$\alpha_0^2\beta_0^1$	26 964	784	47	
26 429	249	137	α_0^4	27 391	1211	22	1211
26 441	261	7	$\alpha_0^1\beta_0^2$	27 425	1245	15	1245
26 465	285	15	$\alpha_0^3\beta_0^1$	27 430	1250	8	1250
26 478	298	2	β_0^3	27 451	1271	29	$1211 + \alpha_0^1$
26 490	310	238	α_0^5	27 487	1307	27	$1245 + \alpha_0^1$
26 501	321	18	$\alpha_0^2\beta_0^2$	27 492	1312	31	$1250 + \alpha_0^1$
26 525	345	18	$\alpha_0^4\beta_0^1$	27 512	1332	50	$1211 + \alpha_0^2$
26 538	358	4	$\alpha_0^1\beta_0^3$	27 549	1369	48	$1245 + \alpha_0^2$
26 550	370	282	α_0^6	27 553	1373	91	$1250 + \alpha_0^2$
26 560	380	31	$\alpha_0^3\beta_0^2$	27 574	1394	95	$1211 + \alpha_0^3$
26 574	394	256	β_0^4	27 610	1430	71	$1245 + \alpha_0^3$
26 585	405	17	$\alpha_0^5\beta_0^1$	27 614	1434	59	$1250 + \alpha_0^3$
26 597	417	5	$\alpha_0^2\beta_0^3$	27 635	1455	159	$1211 + \alpha_0^4$
26 610	430	285	α_0^5	27 670	1490	75	$1245 + \alpha_0^4$
26 620	440	52	$\alpha_0^4\beta_0^2$	27 675	1495	220	$1250 + \alpha_0^4$
26 632	452	5	$\alpha_0^1\beta_0^4$	27 697	1517	229	$1211 + \alpha_0^5$
26 643	463	12	$\alpha_0^6\beta_0^1$	27 730	1550	59	$1245 + \alpha_0^5$
26 655	475	7	$\alpha_0^3\beta_0^3$	27 736	1556	274	$1250 + \alpha_0^5$
26 669	489	223	α_0^8	27 756	1576	258	$1211 + \alpha_0^6$
26 677	497	65	$\alpha_0^5\beta_0^2$	27 790	1610	28	$1245 + \alpha_0^6$
26 689	509	7	$\alpha_0^2\beta_0^4$	27 796	1616	289	$1250 + \alpha_0^6$
26 702	522	9	$\alpha_0^6\beta_0^2$	27 816	1636	223	$1211 + \alpha_0^7$
26 712	532	6	$\alpha_0^4\beta_0^3$	27 849	1669	33	$1245 + \alpha_0^7$
26 727	547	186	α_0^9	27 855	1675	238	$1250 + \alpha_0^7$
26 735	555	76	$\alpha_0^6\beta_0^2$	27 875	1695	205	$1211 + \alpha_0^8$
26 759	579	11	$\alpha_0^8\beta_0^1$	27 913	1733	166	$1250 + \alpha_0^8$
26 768	588	6	$\alpha_0^5\beta_0^3$	27 936	1756	198	$1211 + \alpha_0^9$
26 785	605	146	α_0^{10}	27 971	1791	101	$1250 + \alpha_0^9$
26 791	611	84	$\alpha_0^7\beta_0^2$	27 993	1813	175	$1211 + \alpha_0^{10}$
26 802	622	29	$\alpha_0^4\beta_0^4$	28 028	1848	36	$1250 + \alpha_0^{10}$
26 842	662	78	α_0^{11}	28 050	1870	78	$1211 + \alpha_0^{11}$

[a] α and β are the in-phase and out-of-phase torsions of the C—C bonds connecting the C=O group and the phenyl group.

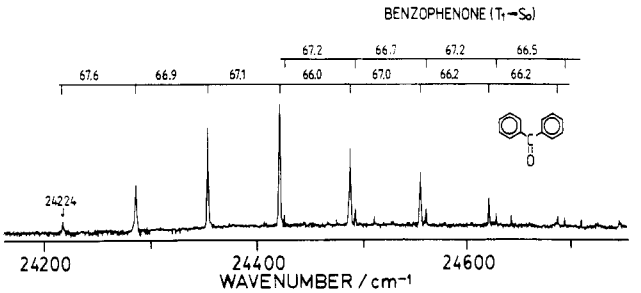

Figure 7. Sensitized phosphorescence excitation spectrum of jet-cooled benzophenone in $T \leftarrow S_0$ region.

(15) Kamei, S.; Sato, T.; Mikami, N.; Ito, M. *J. Phys. Chem.* **1986**, *90*, 5615.

(16) Holtzclaw, K. W.; Pratt, D. W. *J. Chem. Phys.* **1986**, *84*, 4713.

TABLE VI: Phosphorescence Excitation Spectrum of Benzophenone in T ← S_0 Region

ν/ cm^{-1}	$\nu - \nu(0_0^0)$/ cm^{-1}	rel int	assignt[a]	ν/ cm^{-1}	$\nu - \nu(0_0^0)$/ cm^{-1}	rel int	assignt[a]
24 224	0	1	$T_1(n,\pi^*)0_0^0$	25 449	1225	>1	1225
24 292	68	3	α_0^1	25 456	1232	>1	1232
24 359	135	7	α_0^2	25 516	1292	1	$1225 + \alpha_0^1$
24 426	202	9	α_0^3	25 523	1299	1	$1232 + \alpha_0^1$
24 431	207	1	207	25 583	1359	1	$1225 + \alpha_0^2$
24 492	268	5	α_0^4	25 590	1366	1	$1232 + \alpha_0^2$
24 498	274	1	$207 + \alpha_0^1$	25 650	1426	1	$1225 + \alpha_0^3$
24 559	335	4	α_0^5	25 657	1433	1	$1232 + \alpha_0^3$
24 564	340	1	$207 + \alpha_0^2$	25 717	1493	1	$1225 + \alpha_0^4$
24 625	401	2	α_0^6	25 723	1499	1	$1232 + \alpha_0^4$
24 632	408	1	$207 + \alpha_0^3$	25 784	1560	>1	$1225 + \alpha_0^5$
24 691	467	1	α_0^7	25 790	1566	>1	$1232 + \alpha_0^5$
24 698	474	1	$207 + \alpha_0^4$	26 180	1956	25	$S_1(n,\pi^*)0_0^0$

[a] α is the in-phase torsion.

changes from 33° in S_0 to 20° in $S_1(n,\pi^*)$.[15]

Figure 7 shows the sensitized phosphorescence excitation spectrum of jet-cooled benzophenone in the region of the T ← S_0 transition. The intensity of this spectrum is weaker by a factor of 10^3 than the intensity of the $S_1(n,\pi^*) \leftarrow S_0$. Table VI lists the frequencies of the main bands. The spectrum looks very similar to the $S_1(n,\pi^*) \leftarrow S_0$ spectrum. A long progression of the in-phase torsional frequency of 67 cm^{-1} develops from the longest wavelength weak band at 24 224 cm^{-1}, which is tentatively assigned as the origin. A similar progression was also found in the C=O stretching region ($\sim$1230 cm^{-1}), with much weaker intensity than the progression starting from the origin. The close similarity between the T ← S_0 and $S_1(n,\pi^*) \leftarrow S_0$ spectra clearly shows that the excited state associated with the T ← S_0 spectrum is a triplet counterpart ($T_1(n,\pi^*)$) of the $S_1(n,\pi^*)$ state. The frequency separation between the origins of $S_1(n,\pi^*)$ and $T_1(n,\pi^*)$ is 1966 cm^{-1}, which is comparable to 2180 cm^{-1} in the crystal.[17,18] The individual bands of the $T_1(n,\pi^*) \leftarrow S_0$ spectrum are again extremely sharp. The sharp feature is common for the $T(n,\pi^*) \leftarrow S_0$ spectra of all the molecules studied here.

We carefully measured the spectrum to 850 cm^{-1} below the origin of $T_1(n,\pi^*)$ with a hope of finding signals due to $T(\pi,\pi^*)$. However, we could not find any that suggests the existence of $T(\pi,\pi^*)$. In contrast to the cases of benzaldehyde and acetophenone, the vibrational structure of the $T_1(n,\pi^*) \leftarrow S_0$ spectrum is very regular and there is no indication of a perturbation due to a nearby electronic state. Therefore, we think that $T(\pi,\pi^*)$ is located above $S_1(n,\pi^*)$. Batley and Kearns[19] had also attempted in finding $T(\pi,\pi^*)$ for the crystals of benzophenone and 4,4′-diiodobenzophenone. Despite the expected enhancement of the $T(\pi,\pi^*) \leftarrow S_0$ transition for 4,4′-diiodobenzophenone, they failed to find the transition and concluded that $T(\pi,\pi^*)$ is well above $S_1(n,\pi^*)$. The low-field Zeeman experiments of benzophenone in bis(*p*-bromophenyl) ether matrix by El-Sayed and Leyerle[20] also demonstrate that there is no $T(\pi,\pi^*)$ below $S_1(n,\pi^*)$. The fact that no sign was found in our spectrum is consistent with the conclusion obtained by Batley and Kearns and by El-Sayed and Leyerle.

Intersystem Crossing in the Isolated Molecule. All the molecules studied here are very weakly fluorescent, but highly phosphorescent under isolated molecular condition. Their emission properties are qualitatively the same as those in a rigid matrix or crystal. The efficient intersystem crossing from $S_1(n,\pi^*)$ to the triplet manifold is usually explained by the direct spin–orbit coupling between $S_1(n,\pi^*)$ and a lower energy $T(\pi,\pi^*)$, the latter being located near $T(n,\pi^*)$. In the matrix or in the crystal, $T(\pi,\pi^*)$ is reported to lie near $T(n,\pi^*)$ for benzaldehyde and acetophenone, and the energy separation between $S_1(n,\pi^*)$ and $T(n,\pi^*)$ (or $T(\pi,\pi^*)$) is 1500–2000 cm^{-1}. Therefore, intersystem crossing via $T(\pi,\pi^*)$ is highly possible for these molecules in the condensed phase even if the separation between $S_1(n,\pi^*)$ and $T(\pi,\pi^*)$ is small. This is because a statistical limit may be attained for $T(\pi,\pi^*)$ states isoenergetic with $S_1(n,\pi^*)$ owing to the contribution of phonons. It is well-known that phonons play an essential role in intersystem crossing. For example, pyrazine is highly fluorescent and almost nonphosphorescent in the isolated molecule.[21] However, it becomes nonfluorescent or weakly fluorescent and strongly phosphorescent in the crystal, in a matrix, and even in isolated van der Waals complexes.[21] The very efficient intersystem crossing of this molecule in the condensed phase is apparently ascribed to the phonons.

In the cases of the isolated molecules of benzaldehyde, acetophenone, and benzophenone, how we can understand the efficient intersystem crossing? Then, first, we shall examine the triplet-state density. The energy separation between $S_1(n,\pi^*)$ and $T(n,\pi^*)$ of the isolated molecule is 1736, 1488, and 1966 cm^{-1} for benzaldehyde, acetophenone, and benzophenone, respectively. Although $T(\pi,\pi^*)$ could not be located for the isolated molecule, our results suggest that the energy separation between $S_1(n,\pi^*)$ and $T(\pi,\pi^*)$ is not greatly different from that between $S_1(n,\pi^*)$ and $T_1(n,\pi^*)$ for benzaldehyde and acetophenone. Then, it is almost impossible to attain a statistical limit with this small energy separation except for the case where the molecule has very low frequency intramolecular modes in the triplet manifold. The lowest frequency mode is the torsion of the C—C bond(s) connecting the phenyl ring(s) and the C=O group, whose frequency in S_0 is 110, 48, and 57 cm^{-1} for benzaldehyde, acetophenone, and benzophenone, respectively.[9] In $T_1(n,\pi^*)$, it increases to 122,[10] 76, and 67 cm^{-1}, respectively. Corresponding frequencies in $T(\pi,\pi^*)$ are not known, but they will probably not be very different from the values in $T_1(n,\pi^*)$. Given these assumptions, we can estimate the vibrational state density in the triplet manifold by the direct state counting method. In the case of benzaldehyde, the state density of $T(n,\pi^*)$ at an excess vibrational energy of 1500–2000 cm^{-1} is at most 2/cm^{-1}. Even if we add contributions from $T(\pi,\pi^*)$ by assuming the $T(\pi,\pi^*)$ origin at the same energy as the $T(n,\pi^*)$ origin, the state density is only 4/cm^{-1}. In the case of acetophenone, the density increases by the contribution from the internal rotation of the CH_3 group. We calculated the state density of acetophenone with the assumption that the CH_3 group is a free rotor. The calculated density of $T(n,\pi^*)$ at an excess energy isoenergetic with the $S_1(n,\pi^*)$ 0^0 level is at most 20/cm^{-1}. Assuming the same density for $T(\pi,\pi^*)$, the total density is only 40/cm^{-1}. We did not calculate the density for benzophenone because the lack of known vibrational frequencies. However, a dramatic increase of the state density is not expected.

We cannot completely rule out the possibility that $T(\pi,\pi^*)$ is located so far below $S_1(n,\pi^*)$ that a statistical limit is attained at the excess energy isoenergetic with $S_1(n,\pi^*)$. Then, we have to assume $T(\pi,\pi^*)$ is a few thousand cm^{-1} below $T(n,\pi^*)$. Since $T(\pi,\pi^*)$ is located near $T(n,\pi^*)$ in the condensed phase, an enormously large red shift of $T(\pi,\pi^*)$ has to be assumed in going from the condensed phase to the isolated molecule. This is quite unrealistic. Therefore, it seems reasonable that the energy level structure of the isolated molecule is similar to that in the condensed phase. Then, it follows that the vibrational state density should be very small.

A shortage of density of states might be compensated for by a large interaction between $S_1(n,\pi^*)$ and isoenergetic levels in the triplet manifold, whether the interaction is direct spin–orbit or vibrationally induced. However, in order to assure nonrecurrence from the triplet manifold to $S_1(n,\pi^*)$, the interaction region should be very large to span a large number of vibronic levels over a wide energy range. It is difficult to explain why the interaction is

(17) Udagawa, Y.; Azumi, T.; Ito, M.; Nagakura, S. *J. Chem. Phys.* **1968**, *49*, 3764.
(18) Nakahara, A.; Koyanagi, M.; Kanda, Y. *J. Chem. Phys.* **1969**, *50*, 552.
(19) Batley, M.; Kearns, D. R. *Chem. Phys. Lett.* **1968**, *2*, 423.
(20) El-Sayed, M. A.; Leyerle, R. *J. Chem. Phys.* **1975**, *62*, 1579.
(21) Goto, A.; Fujii, M.; Mikami, N.; Ito, M. *J. Phys. Chem.* **1986**, *90*, 2370.

extraordinarily large for these molecules.

Another requirement for efficient intersystem crossing is a large Franck–Condon factor between $S_1(n,\pi^*)$ and isoenergetic vibrational states in $T(n,\pi^*)$ and/or $T(\pi,\pi^*)$. In benzaldehyde, there exists a gross similarity between the vibrational structures of $S_1(n,\pi^*) \leftarrow S_0$ and $T(n,\pi^*) \leftarrow S_0$. However, details are quite different between the two spectra, especially in the low-frequency vibronic bands. In $S_1(n,\pi^*) \leftarrow S_0$, we have fairly strong bands at 137, 191, and 248 cm^{-1}, while there exists only one strong band at 190 cm^{-1} in the corresponding region of the $T_1(n,\pi^*) \leftarrow S_0$ spectrum. This difference strongly suggests that the molecular geometry and potential are greatly different between $S_1(n,\pi^*)$ and $T_1(n,\pi^*)$ along these low-frequency normal coordinates. The spectral differences are more dramatic between the $S_1(n,\pi^*) \leftarrow S_0$ and $T_1(n,\pi^*) \leftarrow S_0$ transitions of acetophenone. Besides the difference due to the internal rotation of the methyl group mentioned before, there is no apparent similarity between the two spectra. In the $S_1(n,\pi^*) \leftarrow S_0$ spectrum, vibrational structure develops up to an excess vibrational energy of 1300 cm^{-1}, but it disappears above 500 cm^{-1} in the $T_1(n,\pi^*) \leftarrow S_0$ spectrum. These facts show that, in addition to the difference in the methyl conformation, the two states are greatly different in their geometry and potential. Such a difference will lead to large Franck–Condon factors between $S_1(n,\pi^*)$ and isoenergetic vibrational levels of $T(n,\pi^*)$ or $T(\pi,\pi^*)$, which contribute to an increase of the intersystem-crossing rate. Especially the low-frequency modes of benzaldehyde and the internal rotation of the methyl group in acetophenone will play a dominant role in the intersystem-crossing process.

In the cases of benzaldehyde and acetophenone, a rationalization for the efficient intersystem crossing despite the small energy gap might be possible by assuming a large Franck–Condon factor and a large value of the interaction matrix element between $S_1(n,\pi^*)$ and $T(\pi,\pi^*)$ or $T(n,\pi^*)$. However, such a reasoning cannot be applied to benzophenone. As we saw before, the $S_1(n,\pi^*) \leftarrow S_0$ and $T_1(n,\pi^*) \leftarrow S_0$ spectra are just duplicates of each other in their vibrational structure. This clearly indicates that $S_1(n,\pi^*)$ and $T_1(n,\pi^*)$ are almost identical in the geometrical structure and potential. Therefore, the Franck–Condon factor should be very small. On the other hand, we have to assume direct intersystem crossing between $S_1(n,\pi^*)$ and $T_1(n,\pi^*)$ because there is no $T(\pi,\pi^*)$ state below $S_1(n,\pi^*)$.[19,20] Then, the interaction matrix element between the two states should be small. Benzophenone has no molecular plane. Therefore, there is no clear distinction between (n,π^*) and (π,π^*). Although the mixing of (n,π^*) and (π,π^*) will increase the interaction matrix element, the close similarity between $S_1(n,\pi^*)$ and $T_1(n,\pi^*)$ suggests a similar mixing ratio for both states, leading to no appreciable enhancement of the interaction matrix element. Therefore, the reasons that might be valid for intersystem crossing in benzaldehyde and acetophenone become invalid for benzophenone. The causes for the efficient intersystem crossing might be different between benzaldehyde or acetophenone and benzophenone. However, in view of the similar emission properties of these three molecules, we feel that the origins for the efficient intersystem crossing are common.

Chemical reaction in $S_1(n,\pi^*)$ or in the triplet states and coupling of the triplet states with highly excited vibrational states in S_0[22] might be considered as origins. Molecular rotation might also play an important role for the efficient intersystem crossing. Potential crossing near $S_1(n,\pi^*)$ might be present, although we have no sign of such a crossing in the observed spectrum. After all, we have no answer to the question of why the intersystem crossing is so efficient in the isolated molecule.

Acknowledgment. We thank T. Azumi, Y. Fujimura, and N. Mikami for stimulating discussions and N. Hirota for helpful advice.

Registry No. Benzaldehyde, 100-52-7; acetophenone, 98-86-2; benzophenone, 119-61-9.

(22) Hochstrasser, R. M.; Scott, G. W.; Zewail, A. H. *Mol. Phys.* **1978**, *36*, 475.

Radical Cations in Pulse Radiolysis of Liquid Alkanes. Time-Resolved Fluorescence Detected Magnetic Resonance†

D. W. Werst and A. D. Trifunac*

Chemistry Division, Argonne National Laboratory, Argonne, Illinois 60439 *(Received: July 28, 1987)*

Alkane and olefin radical cations are characterized by time-resolved fluorescence detected magnetic resonance (FDMR) in pulse radiolysis of neat alkane liquids and binary alkane mixtures at room and low temperatures (~180 K). FDMR–EPR spectra of the *cis*-decalin radical cation and the norbornane radical cation are detected at low concentrations (10^{-3}–10^{-1} M) of *cis*-decalin and norbornane, respectively, in alkane mixtures. Parent minus H_2 olefin radical cations are observed in neat alkanes and in alkane mixtures. Studies of the temperature and concentration dependences of olefin cation formation suggest that olefin cations originate in the fragmentation of parent alkane cations and that this reaction depends on the energy content of the parent cation. Other possible reactions of alkane radical cations are discussed.

1. Introduction

The primary process in alkane radiolysis has long been an intriguing subject of radiation chemistry. Yields of stable products are known for some well-studied cases, but the detailed mechanism for their formation, including the number, identity, and reactions of all the transient species involved, is not yet known. Progress in this area demands a better knowledge of the formation and reactions of the cation/electron pairs and excited states that are produced in the initial excitation event and are responsible for the bulk of the ensuing chemistry.

Alkane radical cation/electron pairs are also progenitors of other transient species such as excited states, ions, and neutral radicals. Their special reactivities make them important reaction intermediates in organic chemistry, and they are responsible for radiation damage in organic materials (polymers, dielectric fluids in electric transformers, living organisms).[1] The great potential of hydrocarbon cations in organic synthesis has only just begun

† Work performed under the auspices of the Division of Chemical Sciences, Office of Basic Energy Sciences of the U.S. Department of Energy.

(1) *Comprehensive Chemical Kinetics*; Bamford, C. H., Tipper, C. F. H., Eds.; Elsevier: New York, 1975; Vol. 14. Garrison, W. M. *Chem. Rev.* **1987**, *87*, 381.

0022-3654/88/2092-1093$01.50/0